Journal of Cellular Biochemistry 93:476–490 (2004)

Differential Transcriptional Effects of PTH and Estrogen During Anabolic Bone Formation

D. von Stechow,[1] D. Zurakowski,[2] A.R. Pettit,[3] R. Müller,[4] G. Gronowicz,[5] M. Chorev,[6] H. Otu,[7] T. Libermann,[7] and Joseph M. Alexander[6]*

[1]Beth Israel Deaconess Medical Center and Harvard Medical School, Boston, Massachusetts
[2]Departments of Orthopaedic Surgery and Biostatistics, Children's Hospital and Harvard Medical School, Boston, Massachusetts
[3]Department of Medicine, New England Baptist Bone and Joint Institute and Harvard Medical School, Boston, Massachusetts
[4]Institute for Biomedical Engineering, ETH and University Zürich, Switzerland
[5]Department of Orthopaedics, University of Connecticut Health Center, Farmington, Connecticut
[6]Bone and Mineral Metabolism Unit, Beth Israel Deaconess Medical Center and Harvard Medical School, Boston, Massachusetts
[7]Genomics Center, Beth Israel Deaconess Medical Center and Harvard Medical School, Boston, Massachusetts

Abstract The aim of this study was to compare transcriptional regulation in vivo during anabolic bone formation induced by either estradiol (E2) treatment or intermittent parathyroid hormone[1-34] (PTH) therapy. We utilized an ovariectomized (OVX) mouse model of osteoporosis and transcriptional profiling to identify genes upregulated by either high-dose E2 or PTH. Five weeks post-OVX, the mice were administered either E2 and/or PTH, or vehicle for 4 weeks. Femoral bones were analyzed by microCT and histomorphometry to confirm the anabolic effect of each treatment. OVX vehicle-treated control mice lost metaphyseal trabecular bone, with significant decrease in trabecular number, thickness, and connectivity. Both E2 and PTH treatments increased trabecular and cortical bone indices above the level of the sham operated controls, fully restoring both bone volume and bone mineral density (BMD). Moreover, PTH/E2 combination treatment led to significantly greater increase in cancellous bone and BMD than would be expected from the additive effects of the separate treatments. To determine whether PTH and E2 treatments were stimulating similar bone anabolic mechanisms, or were activating distinct signaling pathways, we compared patterns of gene expression using transcriptional profiling after either E2 or PTH treatment. After 4, 11, and 24 days of treatment, total RNA was collected from both the distal femoral metaphysis and diaphysis. Transcriptional profiling was performed using Affymetrix GeneChip probe arrays, comprised of approximately 36,000 full-length mouse genes and EST clusters from the UniGene database. Several markers of osteoblast activity, including c-fos, RANKL, PHEX, and PTHR1, were consistently upregulated by PTH in both skeletal sites. PTH treatment also increased expression of Cathespin K, consistent with the predicted increase in osteoclast activity. E2 treatment upregulated a largely distinct set of genes, including TGFβ3, and BMP1, as well as several genes critical for cell cycle control, including Cyclin D1 and CDK inhibitor 1A. Overall, comparison of transcriptional profiles suggest that anabolic responses in bone to PTH and high-dose E2 treatment after OVX-induced osteoporosis involve largely distinct patterns of gene regulation, each resulting in restoration of bone mass. J. Cell. Biochem. 93: 476–490, 2004.

Key words: osteoporosis; synergy; hormone replacement therapy; Swiss-Webster mice; micro-computed tomography; transcriptional profiling

Grant sponsor: National Institutes of Health (to G.G.); Grant number: AR38933; Grant sponsor: National Institutes of Health (to J.M.A.); Grant number: AR47627; Grant sponsor: Arthritis Foundation Postdoctoral Fellowship (to A.R.P.); Grant sponsor: National Health and Medical Research Council C.J. Martin Fellowship (to A.R.P.).

*Correspondence to: Joseph M. Alexander, PhD, Department of Physiology, Tufts University, 136 Harrison Ave, Boston MA 02111. E-mail: Joseph.Alexander@tufts.edu

Received 8 March 2004; Accepted 29 April 2004
DOI 10.1002/jcb.20174

Osteoporosis is considered a global health problem due to the morbidity and mortality associated with fracture [Manolagas and Jilka, 1995; Melton, 1997; Walker-Bone et al., 2001]. Currently approved treatments of osteoporosis act by reducing osteoclast-mediated bone resorption [Greenspan et al., 2000; Lane et al., 2000; Rosen and Bilezikian, 2001]. However, the initial gain in bone mineral density (BMD) associated with these anti-resorptive therapies is due to filling of the remaining remodeling space, rather than actual 'anabolic' bone reconstruction.

In aiming to further improve osteoporosis treatments, much attention has been focused on parathyroid hormone (PTH), which enhances bone formation directly, and has been shown to restore bone mass to normal levels in animal models [Neer et al., 2001]. Several groups have shown the beneficial effect of intermittent PTH administration on both cortical and cancellous bone content [Slovik et al., 1981; Hodsman et al., 1991; Dempster et al., 1993; Baumann and Wronski, 1995; Ejersted et al., 1995; Jerome et al., 1999; Alexander et al., 2001]. Furthermore, the biomechanical strength of femurs and vertebrae assessed by three-point bending and compression tests in PTH-treated animals increased significantly after 8 weeks of treatment [Ejersted et al., 1994, 1995; Hodsman et al., 1997].

Several studies have demonstrated that high dose E2 is anabolic in mice [Bain et al., 1993; Samuels et al., 1999]. When ovariectomized (OVX) Swiss-Webster mice are given lower doses of E2 (more consistent with conventional HRT levels of E2), treatment merely preserves BMD without initiating intermedullary bone formation [Bain et al., 1993]. However, at higher E2 doses, E2 is obviously anabolic and builds bone chiefly by thickening existing trabecular structures in the metaphysis and endosteal cortical thickness at the diaphysis. One of the goals of this study was to utilize large-scale transcriptional profiling to provide insight into gene regulation in response to high dose E2, and the molecular mechanisms that differentiate its effects from those seen with intermittent PTH.

With current osteoporotic treatment regimens preventing only 40–60% of osteoporotic fractures in high-risk patients, the search for novel potent anabolic agents or the combination of both anti-resorptive and anabolic agents to further increase bone mass is ongoing [Cosman et al., 2001]. Combining an anabolic agent like PTH with anti-resorptive agents such as estrogen or bisphosphonates may augment bone mass via divergent mechanisms. However, coadministration of PTH with other agents such as calcitonin [Flicker et al., 1997] or tiludronate [Hodsman et al., 1997] has not always been found to be beneficial in bone mass restoration.

In this study, we carried out transcriptional profiling to explore to what degree there are unique intracellular signaling pathways for E2- and PTH-regulated bone growth, or whether these two treatments activate common anabolic signaling pathways in bone. We utilized microarray RNA profiling to acquire detailed profiles of transcriptional regulation at several timepoints and at both the femoral metaphysis and the diaphysis during the various phases of PTH and E2 anabolic action in bone. The goal of this study was to determine the effects of a combination treatment of 17 beta-estradiol (E2) and PTH (1-34) on the microarchitecture of bone in OVX Swiss-Webster mice, and to identify transcriptional responses during enhancement of bone formation by either agent.

MATERIALS AND METHODS

Animals

Eleven-week-old OVX- or Sham-operated female Swiss-Webster mice were purchased from Taconic Farms (Germantown, NY) and maintained at the animal research facility at the Beth Israel Deaconess Medical Center. Animals were fed Purina Formulab Diet containing 1% Ca (Formulab, Richmond, IN) and water ad libitum throughout the experiment. Mice were sacrificed by CO_2 inhalation.

Experimental Protocol

The experimental protocol was approved by the Institutional Animal Care and Use Committee of the Beth Israel Deaconess Medical Center. The study design is illustrated schematically in Figure 1. The mice were randomly subdivided into six groups of bilaterally OVX and three groups of Sham OVX animals, with 10 animals in each group. A group of each of OVX and Sham animals was sacrificed 1 week postoperatively (T1/OVX and T1/Sham, respectively) and served as baseline controls. Four additional weeks elapsed before initiation of treatment in the remaining groups in order to permit significant bone loss to occur in the OVX

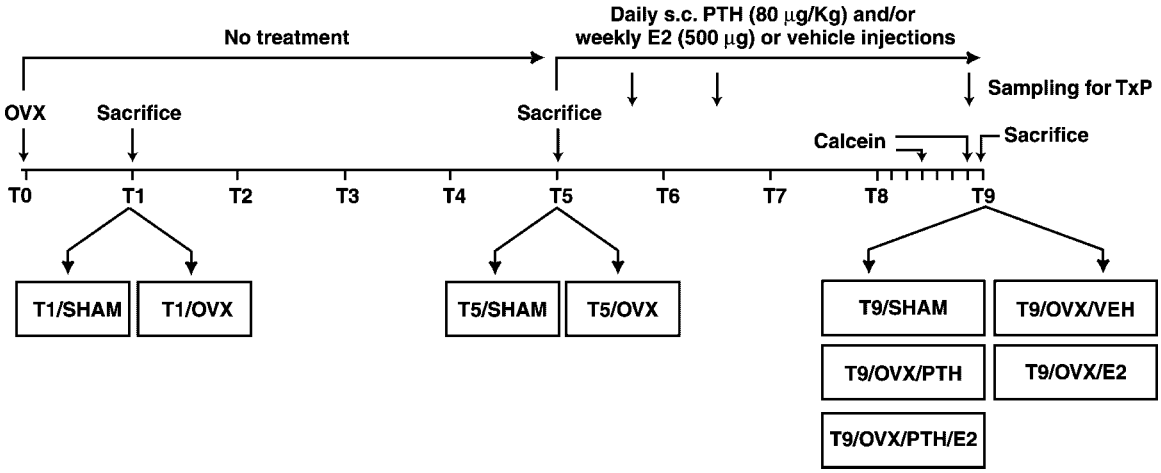

Fig. 1. Schematic representation of experimental design.

animals. At this time, one group of OVX (T5/OVX) and one group of Sham OVX mice (T5/Sham) were sacrificed to evaluate pre-treatment bone loss.

A 4-week daily treatment (5 days a week, Monday–Friday) consisting of s.c. injections of either 80 μg/kg/d of hPTH-(1-34) (Advanced ChemTech, Louisville, KY) and/or 17 beta-estradiol (E2) 500 μg/week (Sigma, St. Louis, MO) or vehicle (sesame oil, Sigma) only was then administered to the respective T9/OVX/PTH and T9/OVX/VEH groups. At the end of the treatment period the animals were sacrificed, together with a 9-week postoperative Sham OVX group (T9/Sham). To label mineralization fronts, all T9 groups were given subcutaneous injections of calcein (15 mg/kg) in 2% sodium bicarbonate solution 3 and 1 day prior to sacrifice. At sacrifice, the femoral bones were separated, cleaned of soft tissues, fixed in 10% phosphate buffered formalin (pH 7.2) for 48 h, and then kept in 70% ethanol until further use.

Micro-Computed Tomography Analysis

For a detailed qualitative and quantitative 3-D evaluation, whole femoral bones were examined by a desktop micro-computed tomography system (μCT 20, Scanco Medical AG, Bassersdorf, Switzerland) equipped with a 10 μm focal spot microfocus X-ray tube as the source [Rüegsegger et al., 1996]. To scan the entire femoral width (3.4–5.1 mm), including the femoral head, a total of 100–150 micro-tomographic slices were acquired at a 34 μm slice increment. Morphometric parameters were determined using a direct 3-D approach in three different pre-selected analysis regions: whole bone (including the articular ends), secondary spongiosa in the distal metaphysis, and diaphyseal cortical bone [Müller et al., 1998; Hildebrand et al., 1999; Alexander et al., 2001].

Histomorphometric Analysis

Following μCT image acquisition, the specimens were dehydrated in progressive concentrations of ethanol, cleared in xylene, and embedded with identical orientation in methylmethacrylate. Longitudinal 5 μM sections from the center of each bone were deplasticized and left unstained for dynamic measurements. To identify osteoclasts, adjacent sections were deplasticized and stained with modified Masson–Goldner Trichrome with Bierbrich Scarlet (Sigma). Histomorphometric analysis was performed using the BioQuant image analysis system (R & M Biometrics, Nashville, TN) with units and measurements according to standardized nomenclature [Parfitt et al., 1987].

Osteocalcin Assay

Blood was sampled prior to sacrifice to determine serum levels of osteocalcin (OC). Serum intact OC was measured by a two-site immunoradiometric assay (IRMA kit, Immutopics, Inc., San Clemente, CA) against the mid-region C-terminal and amino- terminal position of mouse OC with a known sensitivity of 0.1 ng/ml. Intra- and interassay CVs were 2.3 and 4.4%, respectively.

Statistical Analysis

In planning the experiment, a power analysis was performed in order to determine the

sufficient sample size. A total of 90 animals (10 per treatment condition) was required to achieve 90% power ($\alpha = 0.05$, $\beta = 0.10$, effect size = 1.0) to detect significant treatment differences in bone parameters. All continuous variables were checked for normality (Gaussian distribution) using the Kolmogorov–Smirnov test and no skewness was found [Conover, 1999]. Therefore, differences in bone parameters obtained by μCT and histology were evaluated using analysis of variance (ANOVA) with pairwise comparisons tested by the post-hoc Fisher least significant difference (LSD) method. A factorial design (fixed-effects model) was used to test the synergistic effects of the combination treatment. Synergy of the PTH and E2 combination treatment was evaluated using two-way ANOVA and the F-test for comparing slopes. Interaction plots illustrate these relationships [Montgomery, 2001]. Each plot contains two lines: one corresponding to the presence of estrogen (solid line) and the other to no estrogen (dashed line). Presence or absence of PTH is given on the x-axis. A significant F-test indicates a lack of parallelism of the two lines (different slopes) and represents synergy. Data are reported as mean ± standard deviation (SD). Statistical significance was established for two-tailed values of $P < 0.05$.

RNA Isolation From Bone

Swiss-Webster mice used for transcriptional profiling underwent OVX at 11 weeks of age, followed by a 5-week period of osteopenia before beginning either PTH or E2 treatment as described above. At treatment days 4, 11, and 24, femurs were excised from vehicle- E2- or PTH-treated animals (n = 4, per RNA preparation), and separated into metaphyseal and diaphyseal compartments. Bone marrow cells were removed from the diaphysis by flushing with cold PBS. All samples were then immediately snap-frozen in liquid nitrogen. RNA was subsequently extracted from bone samples by homogenization in TRIzol reagent (Life Technologies, Inc., Rockville, MD) according to manufacturer's instructions.

Transcriptional Profiling

Gene expression profiling was performed using Affymetrix GeneChip arrays, essentially as described by the manufacturer (GeneChip Expression Analysis Technical Manual, Affymetrix, Santa Clara, CA). Briefly, first and second strand cDNA were synthesized from 10 μg of total RNA with the SuperScript double stranded cDNA synthesis kit (Life Technologies, Inc.) using poly(T) nucleotide primers. This double stranded cDNA was subsequently used as a template to generate biotinylated cRNA using the BioArray High-Yield T7 RNA transcript labeling kit (Enzo Diagnostics, Farmingdale, NY). Biotin tagged cRNA was fragmented and hybridized for 16 h at 45°C to mouse genome U74v2 oligonucleotide array chips (Affymetrix). The U74v2 set consists of three GeneChip probe arrays, comprised of probe sets from approximately 36,000 full-length mouse genes and EST clusters from the UniGene database. After hybridization the gene chips were washed and stained with streptavidin-phycoerythrin using a GeneChip fluidics workstation 400 (Affymetrix). Affymetrix Microarray Suite 5.0 was used to scan each gene chip and analyze the relative abundance of each gene from the average difference in signal intensities. Quantitative RT-PCR was used to confirm microarray data for selected genes. Genes were annotated using the unchip program (www.unchip.org:8080) and sorted according to function. The rainbow excel macro (Charles Bailey and Towia Libermann) was used to convert numbers into log2 scaled colors.

Real-Time Quantitative RT-PCR

Gene expression was measured by TaqMan real-time PCR according to the manufacturer's protocols (Applied Biosystems, Foster City, CA). For each gene of interest, a set of primers and corresponding internal probe (FAM labeled) were designed using sequences obtained from GenBank and amplicons of 50–70 bp with T_M between 58 and 60°C were selected. Primer and probe (VIC labeled) sets for a reference gene, mouse 18S, were purchased from Applied Biosystems Prior to cDNA synthesis, 2 μg of total RNA was DNase I (Qiagen, Valencia, CA) treated for 15 min at 37°C, after which RNA was reverse-transcribed from random hexamer primers using the Multiscribe Reverse Transcription Kit (Applied Biosystems). PCR reactions were performed using 200 nM of forward and reverse primers together with 100 nM of corresponding probe for both 18S and the target gene of interest on an ABI PRISM 7700 Sequence Detection System (Applied Biosystems) using the following conditions: 2 min at 50°C, 10 min at 95°C, followed by 40 cycles of 95°C for 15 s

and 60°C for 60 s. The number of PCR cycles needed for FAM and VIC fluorescence to cross a threshold of a statistically significant increase in fluorescence (Ct = threshold cycle) was measured using Applied Biosystems software. Relative target gene expression was determined using the formula: Relative Expression = 2 − (CT) where $CT = (Ct_{target}$ gene − $Ct_{reference}$ gene in bone cDNA sample) − (Ct_{target} gene − $Ct_{reference}$ gene in mock reverse transcribed RNA sample).

RESULTS

Effects of OVX on Bone Loss

Consistent with the findings in our previous study [Alexander et al., 2001], μCT and histomorphometric analyses of femoral trabecular and cortical bone showed little change over the duration of the study in any of the structural variables for sham-operated normal Swiss-Webster mice (groups T1/Sham, T5/Sham, T9/Sham). OVX mice demonstrated significantly lower trabecular bone volume density (BV/TV) compared to Sham controls at 1 week ($9 \pm 4\%$ vs. $19 \pm 10\%$, $P < 0.01$), 5 weeks ($5 \pm 3\%$ vs. $21 \pm 11\%$, $P < 0.001$), and 9 weeks ($4 \pm 1\%$ vs. $22 \pm 10\%$, $P < 0.001$). In addition, trabecular thickness, spacing, and number were significantly different in OVX mice compared to Sham controls at 1, 5, and 9 weeks (all $P < 0.05$). However, cortical parameters including total volume, marrow volume/total volume, and thickness were not significantly different between OVX and Sham controls throughout the 9-week study course (all $P > 0.20$). The OVX-induced bone loss was associated with 1.4- and 1.6-fold increases in osteoclast number (N.Oc/BS), quantitated histomorphometrically and observed 1 (T1/OVX) and 5 (T5/OVX) weeks post-OVX (Fig. 3).

Effect of PTH Treatment

At 9 weeks, trabecular bone volume density (BV/TV) in mice treated with PTH alone (T9/OVX/PTH) was 3.5-fold higher than vehicle-treated animals (T9/OVX/VEH) (Table I and Fig. 4). PTH treatment was associated with significant increases in Tb.Th and Tb.N as well as an expected decrease in Tb.Sp. In addition, significant decreases in cortical %MV/TV and increased cortical wall thickness (Ct.Th) were observed at 9 weeks ($P < 0.05$, Table I).

While N.Oc/BS for T9/OVX/VEH (0.86 ± 0.31) and T9/OVX/Sham (0.92 ± 0.39) groups were comparable in magnitude, The number of osteoclasts after 4 weeks of intermittent PTH treatment was slightly elevated (1.19 ± 0.24), but not significantly different compared to T9 OVX and Sham animals (Fig. 3). Trabecular osteoblast and osteoclast surfaces are shown in Table II. Both osteoblast and osteoclast surfaces were significantly higher in T9/OVX/PTH animals compared to T9/Sham and T9/OVX/VEH. No differences were detected between T9/Sham and T9/OVX/VEH regarding observed changes in osteoclast surface.

Mean serum osteocalcin of Sham and OVX treated animals did not change significantly when compared at 1, 5, and 9 weeks, all >0.05. PTH treated mice, however revealed an increase of (231 ± 76 ng/ml) over T9/OVX/VEH animals (137 ± 31 ng/ml, $P < 0.01$, Table II). Serum calcium levels in PTH-treated

TABLE I. Effects of PTH, Estrogen (E2), and Combination of PTH + E2 on Mouse Femurs at 9 Weeks as Determined by μCT[a]

Parameter	OVX	PTH	E2	PTH + E2	PTH vs. OVX *P*-value	E2 vs. OVX *P*-value	PTH + E2 vs. OVX *P*-value
AVD (%)	66 ± 2	74 ± 3	77 ± 4	85 ± 3	<0.001	<0.001	<0.001
Tb.BV/TV (%)	4 ± 1	14 ± 8	34 ± 17	65 ± 16	<0.01	<0.001	<0.001
Tb.Th (mm)	0.06 ± 0.01	0.08 ± 0.01	0.13 ± 0.04	0.22 ± 0.07	<0.05	<0.01	<0.001
Tb.Sp (mm)	0.77 ± 0.20	0.40 ± 0.13	0.29 ± 0.09	0.20 ± 0.08	<0.05	<0.001	<0.001
Tb.N (1/mm)	1.4 ± 0.4	2.8 ± 0.8	3.6 ± 0.8	4.1 ± 0.5	<0.01	<0.001	<0.001
Ct.TV (mm^3)	1.9 ± 0.2	2.0 ± 0.2	1.9 ± 0.2	2.2 ± 0.1	NS	NS	<0.01
Ct.MV/TV (%)	53 ± 6	45 ± 3	48 ± 4	47 ± 7	<0.01	<0.05	<0.05
Ct.Th (mm)	0.25 ± 0.03	0.29 ± 0.01	0.28 ± 0.03	0.36 ± 0.05	<0.01	NS	<0.001

NS, not significant; AVD, (whole femur) apparent volume density; Tb. BV/TV, trabecular bone volume density; Tb.Th, trabecular thickness; Tb.Sp, trabecular spacing; Tb.N, trabecular number; Ct.TV, cortical total volume; Ct.MV/TV, cortical marrow volume density; Ct.Th, cortical thickness.

[a]All Groups were n = 10 Swiss-Webster mice; Data are presented as mean ± standard error. Groups were compared by ANOVA with post-hoc Fisher least significant difference (LSD) method. All *P*-values are two-tailed.

TABLE II. Osteoblast and Osteoclast Surfaces and Osteocalcin Data at 9 Weeks (T9)[a]

Parameter	T9/SHAM	T9/OVX/VEH	T9/OVX/PTH	T9/OVX/E2	T9/OVX/PTH&E2
Ob.S/BS (%)	15.5 ± 4.7	19.6 ± 7.7	41.9 ± 6.8*	27.9 ± 11.3***	17.1 ± 6.8
Oc.S/BS (%)	3.6 ± 0.9	3.0 ± 2.1	6.7 ± 4.4**	4.9 ± 2.8	1.6 ± 1.0****
Osteocalcin (ng/ml)	114 ± 17	137 ± 31	231 ± 76	110 ± 26	172 ± 36

[a]Ob.S/BS (%), osteoblast surface/bone surface; Oc.S/BS (%), osteoclast surface/bone surface. Osteoblast (Ob.S/BS) and osteoclast (Oc.S/BS) surfaces (%) in distal femoral metaphyseal trabecular bone as well as osteocalcin data (ng/ml) of 9-week sham OVX (T9/SHAM), OVX-vehicle treated (T9/OVX/VEH), OVX PTH-treated (T9/OVX/PTH), OVX E2-treated (T9/OVX/E2), and OVX PTH + E2-treated (T9/OVX/PTH + E2) Swiss-Webster mice. Plus-minus values represent the mean ± standard deviation. Groups were compared by ANOVA with post-hoc Fisher least significant difference (LSD) method. All *P*-values are two-tailed.
*$P < 0.001$ versus T9/SHAM and T9/OVX/PTH.
**$P < 0.001$ versus T9/OVX/VEH and T9/OVX/PTH.
***$P < 0.05$ versus T9/SHAM and T9/OVX/E2.
****$P < 0.05$ versus T9/SHAM and T9/OVX/PTH + E2.

mice (9.37 ± 0.27 mg/dl) were slightly elevated, but not significantly different than Sham animals (9.12 ± 0.31 mg/dl) after 4 weeks of treatment.

Effect of Estrogen Treatment

Trabecular BV/TV after 4 weeks of 500 μg/week high-dose E2 (T9/OVX/E2) was increased 8.5-fold over levels in vehicle-treated animals (T9/OVX/VEH) (Table I and Fig. 4). E2 treatment significantly reversed changes in metaphyseal Tb.Th, Tb.Sp and Tb.N, when compared to T9/OVX/VEH animals, (all $P < 0.01$, Table I). While E2 treatment significantly reduced the medullary cavity volume %MV/TV ($P < 0.05$) in comparison to T9/OVX/VEH, it did not produce a significant increase in Ct.Th, suggesting little if any cortical endosteal thickening as seen in PTH-treated mice. Whole bone volume density (AVD) for E2-treated animals was significantly elevated compared to T9/OVX/VEH levels (E2: 77 ± 4% to OVX/VEH: 66 ± 2%, $P < 0.001$) and slightly higher than that seen after PTH treatment alone (PTH: 74 ± 3%, Table I).

N.Oc/BS of E2 treated animals did not exhibit significant changes compared to the levels of Sham control and OVX treated animals at 9 weeks postoperatively (groups T9/OVX/VEH, T9/Sham and T9/OVX/E2, Fig. 3). Changes in osteoclast surface between, T9/OVX/VEH and T9/OVX/E2 were not significantly different. However, osteoblast surface was significantly higher in T9/OVX/E2 than in T9/Sham, but not in comparison to T9/OVX/VEH.

Mean serum osteocalcin levels in E2 treated animals (110 ± 26 ng/ml) did not show significant differences compared to OVX (137 ± 31 ng/ml) and Sham control animals (114 ± 17 ng/ml) at 9 weeks (all $P > 0.05$, Table II).

Effects of PTH + E2 Combination Treatment

The combination treatment of PTH+E2 (T9/OVX/PTH + E2) demonstrated a 16-fold increase over vehicle-treated animals (T9/OVX/VEH) for trabecular BV/TV after 4 weeks (Table I and Fig. 4). PTH + E2 treatment significantly reversed the findings for Tb.Th, Tb.Sp and Tb.N when compared to T9/OVX/VEH (all $P < 0.001$, Table I).

Cortical parameters revealed a significant increase for Ct.TV and Ct.Th over T9/OVX/VEH, as well as a significant reduction of the medullary cavity volume %MV after PTH + E2 treatment (all $P < 0.05$, Table I).

Whole bone parameters (AVD) in animals treated with PTH + E2 revealed a significant increase in volume density, not only compared to the OVX group (85 ± 3% vs. 66 ± 2%, $P < 0.001$), but also compared to PTH (74 ± 3%) and E2 (77 ± 4%) individual treatments (Table I).

In the PTH + E2 treatment group (group T9/OVX/PTH + E2, Fig. 3), the N.Oc/BS decreased by nearly 50% when compared to Sham control levels at 9 weeks postoperatively. Osteoclast surface was significantly lower in T9/OVX/PTH + E2 compared to T9/Sham ($P < 0.05$, Table II). In contrast, Ob.S/BS was similar in T9/Sham control compared to the T9/OVX/PTH + E2 treatment group. However, in OVX mice, T9/OVX/PTH and T9/OVX/E2 significantly increase % Ob.S/BS (Table II).

Mean serum osteocalcin levels after PTH + E2 treatment (172 ± 36 ng/ml) were significantly higher than OVX ($P < 0.05$), and Sham control animals ($P < 0.001$) at 9 weeks. In addition, the osteocalcin levels in the combined PTH + E2 treatment was significantly higher than the mean serum level after E2 treatment

($P < 0.001$) and significantly lower than after PTH treatment ($P < 0.01$, Table II).

Synergistic Effects of the Combination Treatment

As in many experiments involving 2×2 factorial designs, we examined the magnitude and direction for individual and combined treatment effects of PTH and E2 on trabecular bone obtained by μCT measurements. Compared to OVX mice, BV/TV was increased 3-fold by PTH treatment and 8-fold by E2 treatment. The combination treatment of PTH + E2 produced an increase in BV/TV of greater than 16-fold. This is illustrated by the interaction plot in Figure 2A, where the significant F-test ($P < 0.01$) signifies non parallel lines. As evident by the empirical data shown in this figure, OVX-vehicle animals had a mean BV/TV level of 4%, whereas those treated with PTH had 14% (dashed line). Estrogen treatment alone was associated with a BV/TV level of 34%, whereas animals that received the PTH + E2 combination exhibited a mean level of 65% (solid line).

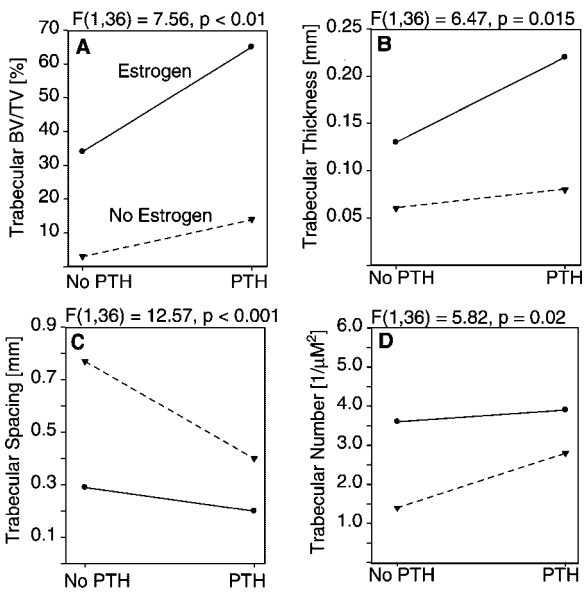

Fig. 2. Interaction plots presenting the empirical data for individual and combined treatments of PTH and estrogen on trabecular bone. Effects are shown for (**A**) trabecular bone volume density (BV/TV), (**B**) trabecular thickness, (**C**) trabecular spacing, and (**D**) trabecular number. Each plot contains two lines: one corresponding to the presence of estrogen (solid line) and the other to no estrogen (dashed line). Presence or absence of PTH is given on the x-axis. The symbols at the end of each line denote means. As shown by the non parallel lines in each plot, synergy was achieved for all the illustrated outcome parameters.

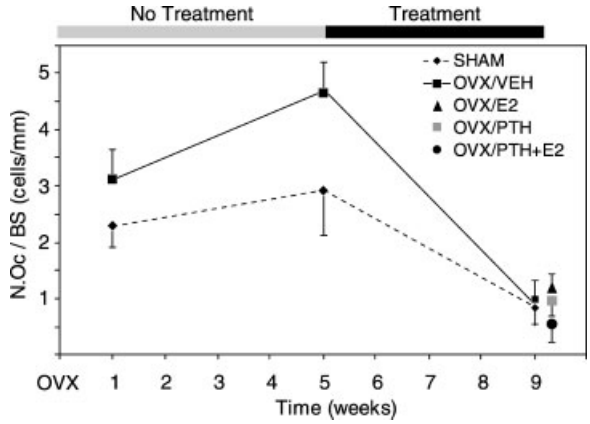

Fig. 3. Oc.N/BS in femoral distal metaphyseal trabecular bone of Swiss-Webster mice. Groups were compared by ANOVA with post-hoc Fisher least significant difference (LSD) method. All *P*-values for all 9-week control and treatment groups are two-tailed.

Tb.Th increased 1.3-fold by PTH treatment and 2.2-fold by E2 treatment. The combination treatment of PTH+E2 produced an increase in Tb.Th of 3.7-fold. The F-test ($P = 0.015$) in Figure 2B represents a significant difference in slopes (lack of parallelism). In the case of Tb.Sp, PTH treatment showed a decrease of 1.5-fold, whereas E2 showed a decrease of 1.6-fold. The combination treatment of PTH + E2 produced a decrease of 1.8 fold. Unlike in the previous interaction plots, the solid line representing estrogen is at the bottom, whereas the dashed line representing no estrogen is at the top. The highly significant F-test ($P < 0.001$) can be appreciated by the nonparallel slopes of the two lines (Fig. 2C).

Although the differences in magnitude for Tb.N among the different treatments is subtler than the effects on other trabecular parameters, the combination therapy still reached synergy (F-test, $P = 0.02$). PTH treatment alone doubled the mean level for Tb.N (2.8 mm^{-1}) compared to the Tb.N in OVX-vehicle treated mice (1.4 mm^{-1}, dashed line). E2 treatment increased the mean level of Tb.N 2.6-fold (3.6 mm^{-1}), and the combined treatment of PTH + E2 (solid line) increased it by nearly 3-fold (4.1 mm^{-1}, Fig. 2D).

Genes Regulated by PTH or E2 Treatment in Bone

For PTH or E2 transcriptional profiling studies, Swiss-Webster mice underwent the same OVX protocol described in Figure 1. Femurs were excised from experimental animals after 4, 11, or 24 days of PTH (80 μg/kg/day)

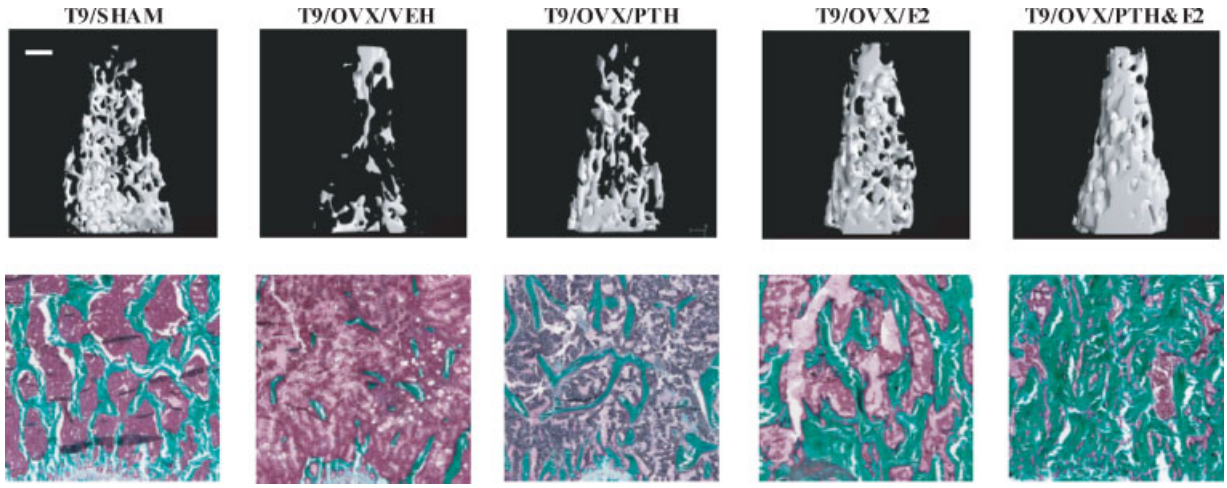

Fig. 4. 3-D μCT images (top, bar = 1 mm) and photomicrographs (bottom, Mason–Goldner Trichrome and Bierbrich Scarlet) of equivalent regions of distal femoral metaphyseal trabecular bone of 9 week Sham, OVX-VEH-treated, OVX PTH treated, OVX E2 treated, and OVX PTH & E2 treated Swiss-Webster mice. Photomicrographs were taken in the same region below the epiphysial growth plate (bottom). Images were obtained from animals with median cancellous BV/TV values. [Color figure can be viewed in the online issue, which is available at www.interscience.wiley.com.]

or E2 (500 μg/week) treatment, and separated into metaphyseal and diaphyseal compartments. For this initial analysis of microarray data, we employed strict criteria for inclusion in this candidate gene list, which were as follows: (1) all candidates had an absolute signal intensity >0.5 (where 1.0 is the median signal intensity on the chip); this criterion excludes low intensity gene signals that may exhibit large changes in regulation due to low baseline signal/noise values, (2) all candidate genes were required to exhibit at least a 2-fold upregulation at all timepoints and at both the femoral metaphysis and diaphysis bone sites; this additional criterion excludes gene candidates that may only be upregulated in either the metaphysis or diaphysis at a specific timepoint—thus our analysis may have dropped several important early-intermediate regulated genes, but also excludes false positives that were not found to be regulated at more than one bone site or experimental timepoint. Figures 5 and 6 show a partial list of regulated genes of interest for PTH and E2, respectively. Among the PTH-regulated genes listed are vitamin D receptor, Rank ligand, and Cathepsin K. For E2 regulated genes, several intriguing candidates were consistently upregulated at all timepoints and in both metaphysis and diaphysis, including Bcl2-associated Bag3 (an anti-apoptotic protein), BMP1 and BMP8a, cyclin D1, PTHR1, and cathepsin L.

In order to verify the results obtained from this iterative microarray analysis, the mRNA levels of four regulated genes were analyzed using real-time PCR and RNA from either PTH- or E2-treated metaphysis at 4, 11, and 24 days. Gene expression was measured by TaqMan real-time PCR. Figures 5 and 6 show Taqman results from PTH and E2 treated metaphyseal RNA, respectively. Metaphyseal RNA samples from PTH-treated mice consistently showed elevated RNA levels of Rank ligand (RankL) and vitamin D receptor (VDR) at all three timepoints tested by real time Taqman PCR, while PTHR1 and Rank RNAs showed no altered expression as a result of PTH treatment (Fig. 5). Metaphyseal RNA samples from E2-treated mice consistently showed elevated RNA levels of PTHR1 at all three timepoints tested by real time Taqman PCR, while RankL, VDR and Rank RNAs showed no altered expression as a result of E2 treatment (Fig. 6).

We next examined a subset of common genes that were upregulated in response to either PTH or E2 treatment in the distal metaphysis (Fig. 7). Criteria for inclusion in this list of common genes were identical to that listed above. Microarray data from metaphyseal bone RNA after E2 treatment indicated that a total of 816 genes were significantly upregulated at all three timepoints examined, while PTH treatment increased gene expression of 440 genes. Of these, 65 genes were upregulated by both

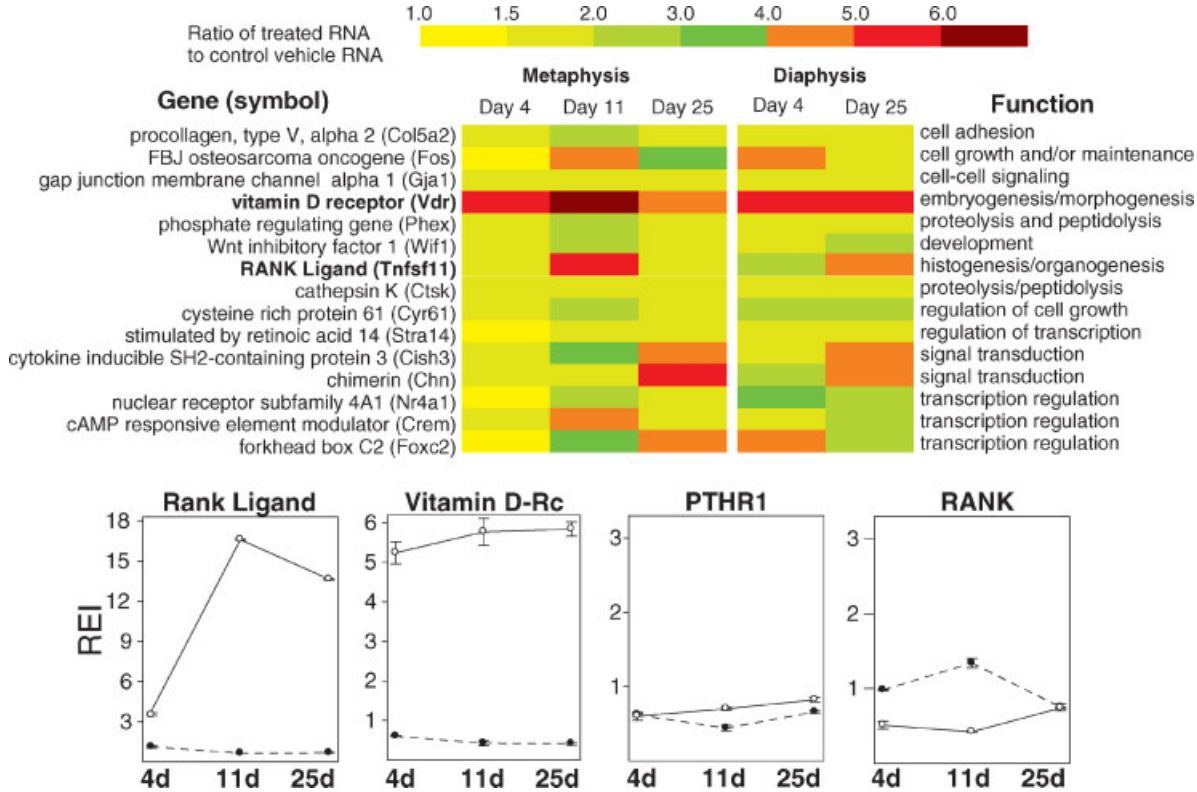

Fig. 5. Microarray data and real-time Taqman PCR of specific gene targets from PTH-treated metaphysis. Based on microarray results shown above, RANKL and VDR were predicted to be upregulated by PTH, a finding confirmed by Taqman PCR. PTHR1 and RANK were also examined by Taqman as controls, because there was no evidence of regulation of either gene in microarrays, a finding also confirmed by PCR.Taqman results are expressed as relative expression intensity. Dashed lines represent QPCR data from vehicle-treated animals, while solid lines represent E2-treated animals. [Color figure can be viewed in the online issue, which is available at www.interscience.wiley.com.]

treatments, 20 of them of unknowns or of unknown function. These common genes represent a small fraction of the total genes upregulated by E2 (15%) or PTH (8%). We hypothesized that many of these loci will represent bone matrix structural proteins that make up nascent osteoid, and other functional proteins critical for new bone formation, regardless of the anabolic treatment. Figure 7 displays these data—categorized by cellular location—as well as a list of known structure proteins that are found to be commonly upregulated by either PTH or supraphysiologic E2 administration.

DISCUSSION

The aim of this study was to investigate the effects of a PTH and E2 combination treatment in OVX Swiss-Webster mice compared to either of the treatment regimes alone, and to document changes in gene expression by microarray analysis after PTH or E2 administration. The most important findings of this study revealed, (1) a combination treatment resulted in a marked overall increase of cancellous bone and (2) this treatment regimen exhibited synergistic effects, indicating that the combination therapy produced a significantly greater result than would be expected from adding together their separate effects.

We selected the Swiss-Webster outbred strain over other strains for its substantial amount of trabecular bone in its femoral metaphyses and a quantifiable loss of both cancellous and cortical bone within 4–5 weeks following OVX [Bain et al., 1993]. Using this model, we have consistently observed bone loss associated with increased osteoclast numbers within 1-week post-OVX. This increase in osteoclast activity results in the marked bone loss observed at 5 weeks. Osteoclast numbers decline to Sham-OVX control levels by 9 weeks postoperatively, when further bone loss is minimal, and are unaffected by the intermittent PTH treatment. The changes in osteoclast numbers and bone loss are similar to results found in post-OVX

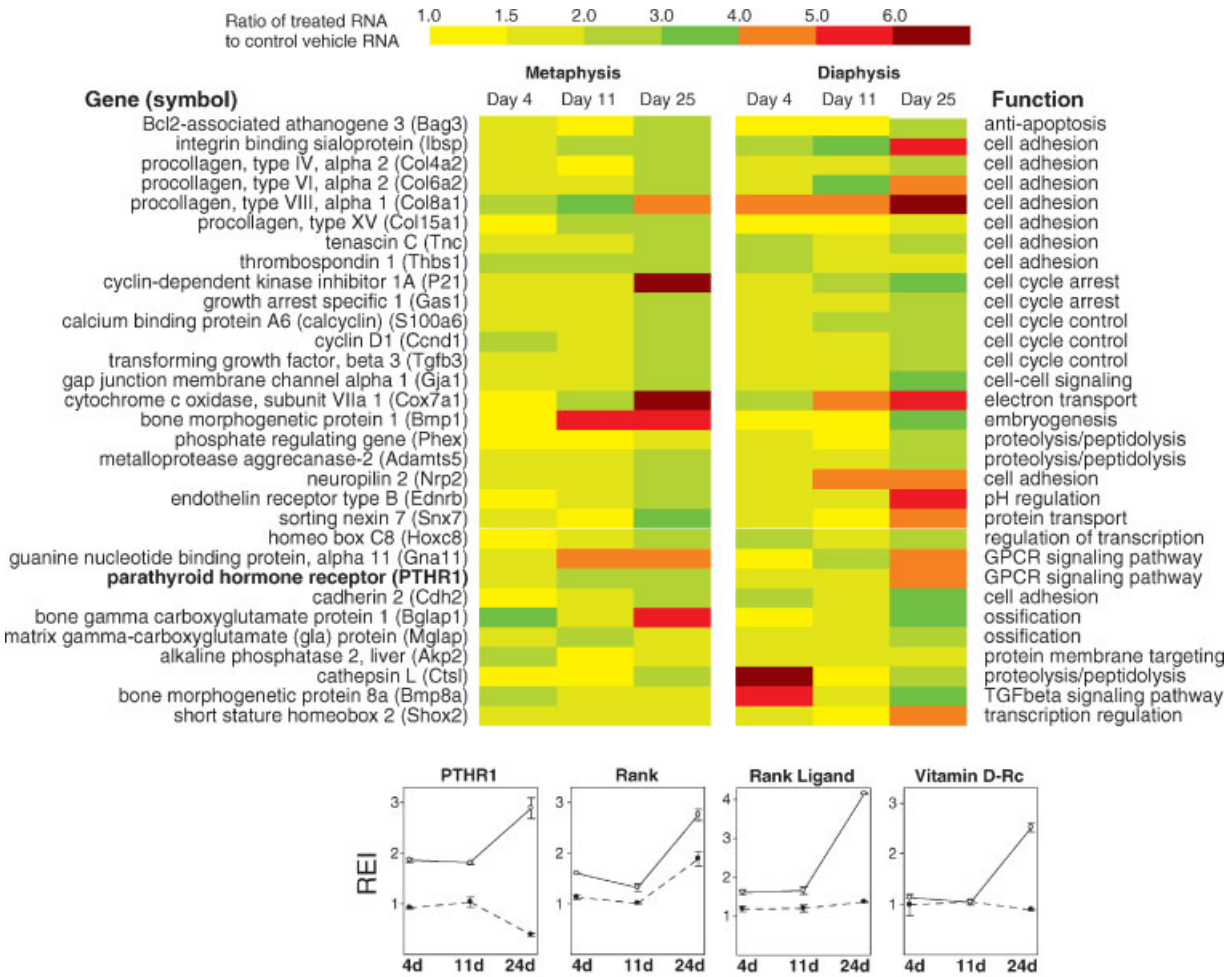

Fig. 6. Microarray data and real time Taqman PCR of specific gene targets from E2-treated Metaphysis. Based on microarray results, PTHR1, RANKL, VDR, and RANK were examined by Taqman. RANKL, VDR, and RANK were used as controls, and were examined by Taqman because there was no consistent regulation of either gene in microarrays in all timepoints examined, a finding also confirmed by PCR. However, note the upregulation of both RankL and VDR at 24 days E2 treatment. This finding is consistent with microarray results, which showed increases in gene expression of both genes only at 24 days (data not shown). Taqman results are expressed as relative expression intensity. Dashed lines represent QPCR data from vehicle-treated animals, while solid lines represent E2-treated animals. [Color figure can be viewed in the online issue, which is available at www.interscience.wiley.com.]

follow-up in rats [Li et al., 1997; Baldock et al., 1998].

Overall, the Swiss-Webster mouse model is consistent with results obtained from studies in other rodents and humans [Dempster et al., 1993; Lindsay et al., 1997; Shen et al., 2000]. In this study, we show that the increase in trabecular bone volume density in this model after combination therapy consists of both, a doubling of Tb.N (~100%) and to a lesser degree an increase of Tb.Th (~33%). The increases in Tb.Th and Tb.N suggest that the anabolic effect of PTH is brought about by both thickening and further tunneling of existing trabeculae and the resulting amplification of the trabecular density appears to occur consequent to large increases in osteoblast number and activity. Reported findings in humans also revealed a similar increase in Tb.N, however, no change or even a small decrease in Tb.Th [Reeve et al., 1980; Hodsman et al., 2000]. These results are in contrast to the rescue of trabecular bone volume density in rats, where it is mainly attributable to an increase in Tb.Th (~100% reversal) [Meng et al., 1996]. Another important feature of this mouse model is the effect of PTH action on cortical bone, again providing striking similarities between this animal model and findings in humans [Cann et al., 1999]. We observed a decrease of Ct. %MV in T9/OVX/PTH mice when

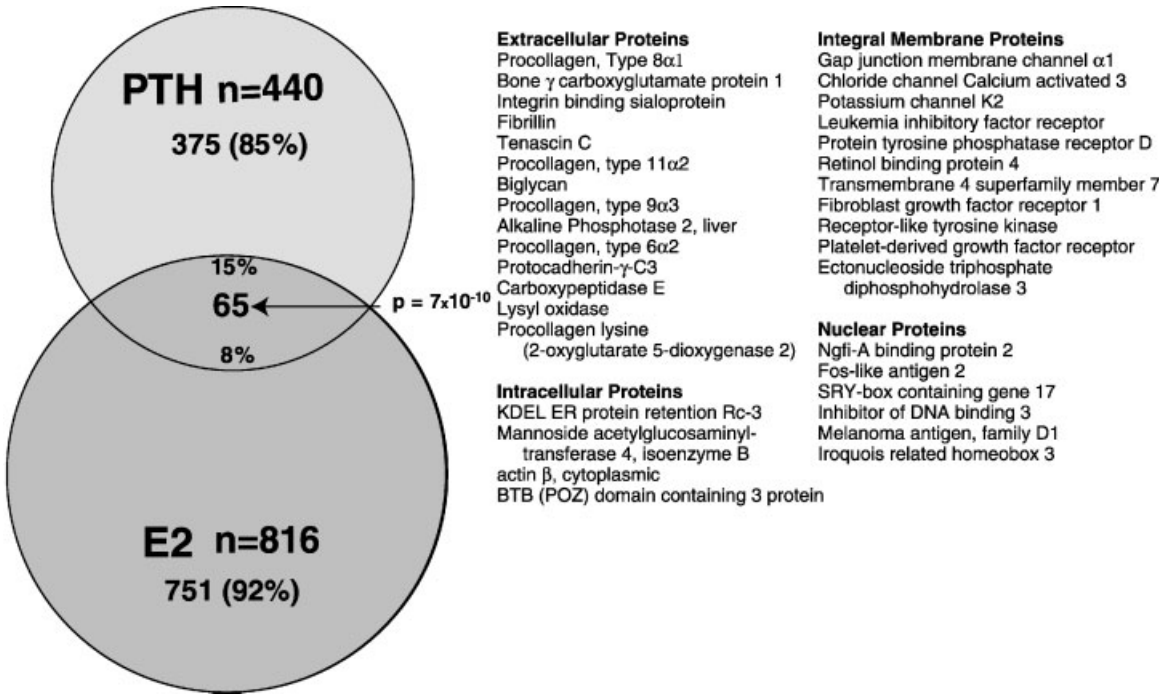

Fig. 7. Comparison of gene expression patterns at the distal femoral metaphysis for both PTH and E2-treated mice reveals a distinct subset of genes upregulated by both anabolic treatments. *P* is the probability index that such an overlapping pattern would occur randomly. A list of 35 known genes included in the common loci are listed on the right.

compared to T9/OVX/VEH animals, while at the same time cortical thickness and overall cortical volume increased by the same magnitude. Taken together, the Swiss-Webster mouse model employed in this study closely resembles the findings in humans. Nevertheless, neither the rat or mouse models display cortical haversian remodeling as it is seen in humans.

The unique effect of supraphysiologic estrogen treatment on long bones in mice, leading to an osteosclerosis-like appearance of the medullary cavity, has been described in several studies [Bain et al., 1993; Samuels et al., 1999]. Such a degree of cancellous bone formation after estrogen administration in mammals has only been observed in mice [Simmons, 1966], and then only when the dose of E2 administered exceeds physiological relevant levels by more than a factor of 100. The effect of estrogen on bone in rats is limited to cancellous bone, occurs at much lower doses and decreases with age in contrast to the effect of estrogen in mice [Turner et al., 1999]. The dose of 500 μg/week E2 in this study was based on previous studies of Swiss-Webster mice reporting maximal stimulation of bone formation with this dose [Bain et al., 1993], with the hypothesis that such a supraphysiologic dose would cause maximal stimulation of E2-regulated gene expression. At the same time, by employing such a treatment the rate of bone resorption in OVX animals decreased and the rate of bone formation increased to a level equivalent of that seen in Sham-operated animals. The findings in our study are in good agreement with results reported by Bain et al. [1993] where all parameters of full and cancellous bone in the E2-treated animals reached or even surpassed the level of Sham controls, while the cortical parameters were almost identical in these two groups.

The mechanisms responsible for the remarkable effects of estrogen on bone in some animal models have been a matter of intense debate. One issue has been whether the anti-resorptive activity of estrogen can be considered a major factor in the estrogen induced bone formation in growing mice, [Simmons, 1966]. In contrast to studies in rats [Westerlind et al., 1993; Sims et al., 1996], we found a significant effect of estrogen on osteoblast perimeter (80% increase of Ob.S/BS in E2-treated compared to Sham-treated animals), a doubling in BFR (data not

shown) and a small, nonsignificant decrease in serum osteocalcin ($P > 0.05$). However, target cells and the role of estrogen in mediating the induction of bone formation in mice was not determined.

While physiologic serum levels of E2 clearly impact bone homeostasis by inhibiting bone resorption, much of its mode of action is likely to be receptor-mediated locally in osteoblast and stromal cell types. Estrogen has been shown to downregulate programmed apoptosis in osteoblasts at least in part by preventing the downregulation of bcl-2 levels seen after OVX [Gohel et al., 1999]. One model of E2 + PTH anabolic action hypothesizes that E2 prolongs the cellular half-life of osteoblasts that are then further stimulated by intermittent PTH treatment. The majority of this regulation is presumed to be mediated via two intracellular estrogen receptors, ERα and ERβ, both members of the steroid receptor superfamily, which are encoded by separate genes located on different chromosomes. The expression of each ER isoform appears to be differently regulated during osteoblast differentiation [Bland, 2000]. Ishibashi et al. [1998] reported decreases of ERβ mRNA expression in MC3T3-E1 cells during osteoblast maturation, while ERα is correlated with increasing osteoblast differentiation in rat calvarial cells [Bodine et al., 1998]. The findings in human SV-HFO cells differ in that higher expression of ERβ is seen with increased differentiation, with mRNA levels of ERα remaining relatively constant [Arts et al., 1997].

In the combination PTH + E2 treated animals, the augmentation of trabecular bone was due to an overall increase in BV/TV, almost doubling the effect of E2 and increasing nearly 6-fold compared to PTH treatment. These mice exhibited enhanced Tb.Th as well as TbN, of which the latter is not seen in rats. In addition, the combination treatment caused a significant increase in Ct.Th. This finding differs from reported rat data, where Ct.Th is increased at the expense of an ~15-fold increase of cortical porosity when compared to OVX vehicle treated animals [Zhou et al., 2001]. There is some evidence in the literature that an interaction between PTH and estrogen exists in osteoblasts [Rao et al., 1994; Kudo et al., 1995], however the underlying mechanism has not been defined. For example Nasu et al. [2000] have demonstrated that PTH stimulates alkaline phosphatase (ALP) activity and collagen synthesis by osteoblasts only after pretreatment with E2. The synergistic effects of the PTH + E2 combination treatment in this study indicate that this could be a promising modality for future treatments of osteoporosis. Clearly however, this treatment regimen requires further investigation.

In this study, transcriptional profiling has identified a short list of important regulatory proteins, and real-time PCR is in agreement with microarray analysis. Among the PTH-regulated genes listed are c-fos, vitamin D receptor, Phex, Rank ligand, and Cathepsin K [Müller et al., 1998; Balto et al., 2000]. The protooncogene c-fos and other activating protein 1 family members are critical transcriptional mediators in bone, and knockout mice (c-fos −/−) fail to respond to intermittent PTH [Fujita et al., 2002]. There is also ample in vitro evidence that PTH increases expression of VDR and RANKL [Huening et al., 2002; Locklin et al., 2003]. For E2 regulated genes, several intriguing candidates were consistently upregulated at all timepoints and in both metaphysis and diaphysis, including Bcl2-associated Bag3 (an anti-apoptotic protein) [Gohel et al., 1999], BMP1 and 8a, cyclin D1, PTHR1, and cathepsin L. In primary OBs derived from transgenic rats harboring a dominant negative ER mutant, cyclin D1 and D2 mRNAs are downregulated when compared with wildtype littermates, suggesting a role for E2 in regulating cyclins, and potentially OB proliferative rates [Fujita et al., 2002].

Taking into account the mouse-specific response to estrogen and the fact that the OVX rat animal model traditionally has been the most commonly used in vivo model for evaluating anti-osteoporotic activity of both anabolic and anti-resorptive agents, questions regarding the relevance of an OVX mouse model arise. Although the number of studies in the literature involving OVX mice is still rather small, they consistently report bone loss and an increase in bone resorption following OVX, similar to the bone loss seen in estrogen-depleted women. Furthermore, in contrast to the rat model, the availability of numerous outbred mouse strains with differences in peak bone mass and their susceptibility to bone loss following OVX, offer unique opportunities to study the polygenic nature of osteoporosis. In addition, gene manipulation and homologous recombination (knockout) technologies have been used extensively for

the study of genes involved in the pathogenesis of, and potential therapies for, osteoporosis [Kong et al., 1999; Ducy et al., 2000; Montero et al., 2000]. This OVX Swiss-Webster mouse model offers an opportunity to introduce genetic modifications into a valid animal model for osteoporosis, thus enabling investigation of possible molecular mechanisms involved in the effect of anabolic and anti-resorptive agents on the osteoporotic skeleton.

By examining site-specific transcriptional regulation at several timepoints over the course of PTH or E2 treatment, we have begun to catalog a more complete description of critical genes regulated during osteoblast and osteoclast differentiation, with the ultimate goal of identifying novel osteoblast-specific genes and critical regulators of the observed anabolic growth of bone. Our profiling results thus far confirm that important bone regulatory molecules, such as vitamin D receptor (VDR), RANKL, PTHR1, AP-1 and cathespin K, exhibit upregulation in vivo in response to these treatments. These findings have been confirmed for a subset of identified genes by subsequent real-time PCR. These data increase our confidence that such a strategy can be used to build a physiologically relevant picture of the multitude of regulatory pathways involved in anabolic bone growth.

ACKNOWLEDGMENTS

The authors thank Gary Hattersley PhD and Jack Green PhD for their helpful discussions regarding the microarray and real-time PCR data.

REFERENCES

Alexander JM, Bab I, Fish S, Müller R, Uchiyama T, Gronowicz G, Nahounou M, Zhao Q, White DW, Chorev M, Gazit D, Rosenblatt M. 2001. Human parathyroid hormone 1-34 reverses bone loss in ovariectomized mice. J Bone Miner Res 16:1665–1673.

Arts J, Kuiper GG, Janssen JM, Gustafsson JA, Lowik CW, Pols HA, van Leeuwen JP. 1997. Differential expression of estrogen receptors alpha and beta mRNA during differentiation of human osteoblast SV-HFO cells. Endocrinology 138:5067–5070.

Bain SD, Bailey MC, Celino DL, Lantry MM, Edwards MW. 1993. High-dose estrogen inhibits bone resorption and stimulates bone formation in the ovariectomized mouse. J Bone Miner Res 8:435–442.

Baldock PA, Morris HA, Need AG, Moore RJ, Durbridge TC. 1998. Variation in the short-term changes in bone cell activity in three regions of the distal femur immediately following ovariectomy. J Bone Miner Res 13: 1451–1457.

Balto K, Müller R, Carrington DC, Dobeck J, Stashenko P. 2000. Quantification of periapical bone destruction in mice by micro-computed tomography. J Dent Res 79: 35–40.

Baumann BD, Wronski TJ. 1995. Response of cortical bone to antiresorptive agents and parathyroid hormone in aged ovariectomized rats. Bone 16:247–253.

Bland R. 2000. Steroid hormone receptor expression and action in bone. Clin Sci (Lond) 98:217–240.

Bodine PV, Henderson RA, Green J, Aronow M, Owen T, Stein GS, Lian JB, Komm BS. 1998. Estrogen receptor-alpha is developmentally regulated during osteoblast differentiation and contributes to selective responsiveness of gene expression. Endocrinology 139:2048–2057.

Cann CE, Roe EB, Sanchez SD, Arnaud CD. 1999. PTH effects in the femur: Envelope specific responses by 3DQCT in postmenopausal women. J Bone Miner Res 14:S137.

Conover WJ. 1999. "Practical nonparametric statistics." New York: John Wiley & Sons.

Cosman F, Nieves J, Woelfert L, Formica C, Gordon S, Shen V, Lindsay R. 2001. Parathyroid hormone added to established hormone therapy: Effects on vertebral fracture and maintenance of bone mass after parathyroid hormone withdrawal. J Bone Miner Res 16:925–931.

Dempster DW, Cosman F, Parisien M, Shen V, Lindsay R. 1993. Anabolic actions of parathyroid hormone on bone. Endocr Rev 14:690–709.

Ducy P, Amling M, Takeda S, Priemel M, Schilling AF, Beil FT, Shen J, Vinson C, Rueger JM, Karsenty G. 2000. Leptin inhibits bone formation through a hypothalamic relay: A central control of bone mass. Cell 100: 197–207.

Ejersted C, Andreassen TT, Nilsson MH, Oxlund H. 1994. Human parathyroid hormone(1-34) increases bone formation and strength of cortical bone in aged rats. Eur J Endocrinol 130:201–207.

Ejersted C, Andreassen TT, Hauge EM, Melsen F, Oxlund H. 1995. Parathyroid hormone (1-34) increases vertebral bone mass, compressive strength, and quality in old rats. Bone 17:507–511.

Flicker L, Hopper JL, Larkins RG, Lichtenstein M, Buirski G, Wark JD. 1997. Nandrolone decanoate and intranasal calcitonin as therapy in established osteoporosis. Osteoporos Int 7:29–35.

Fujita M, Urano T, Horie K, Ikeda K, Tsukui T, Fukuoka H, Tsutsumi O, Ouchi Y, Inoue S. 2002. Estrogen activates cyclin-dependent kinases 4 and 6 through induction of cyclin D in rat primary osteoblasts. Biochem Biophys Res Commun 299:222–228.

Gohel A, McCarthy MB, Gronowicz G. 1999. Estrogen prevents glucocorticoid-induced apoptosis in osteoblasts in vivo and in vitro. Endocrinology 140:5339–5347.

Greenspan SL, Harris ST, Bone H, Miller PD, Orwoll ES, Watts NB, Rosen CJ. 2000. Bisphosphonates: Safety and efficacy in the treatment and prevention of osteoporosis. Am Fam Physician 61:2731–2736.

Hildebrand T, Laib A, Müller R, Dequeker J, Rüegsegger P. 1999. Direct three-dimensional morphometric analysis of human cancellous bone: Microstructural data from spine, femur, iliac crest, and calcaneus. J Bone Miner Res 14: 1167–1174.

Hodsman AB, Steer BM, Fraher LJ, Drost DJ. 1991. Bone densitometric and histomorphometric responses to sequential human parathyroid hormone (1-38) and salmon calcitonin in osteoporotic patients. Bone Miner 14:67–83.

Hodsman AB, Fraher LJ, Watson PH, Ostbye T, Stitt LW, Adachi JD, Taves DH, Drost D. 1997. A randomized controlled trial to compare the efficacy of cyclical parathyroid hormone versus cyclical parathyroid hormone and sequential calcitonin to improve bone mass in postmenopausal women with osteoporosis. J Clin Endocrinol Metab 82:620–628.

Hodsman AB, Kisiel M, Adachi JD, Fraher LJ, Watson PH. 2000. Histomorphometric evidence for increased bone turnover without change in cortical thickness or porosity after 2 years of cyclical hPTH(1-34) therapy in women with severe osteoporosis. Bone 27:311–318.

Huening M, Yehia G, Molina CA, Christakos S. 2002. Evidence for a regulatory role of inducible cAMP early repressor in protein kinase a-mediated enhancement of vitamin D receptor expression and modulation of hormone action. Mol Endocrinol 16:2052–2064.

Ishibashi O, Saitoh Y, Hara K, Kawashima H. 1998. Estrogen receptors alpha and beta are differentially expressed during osteoblast maturation. Bone 23:F043.

Jerome CP, Johnson CS, Vafai HT, Kaplan KC, Bailey J, Capwell B, Fraser F, Hansen L, Ramsay H, Shadoan M, Lees CJ, Thomsen JS, Mosekilde L. 1999. Effect of treatment for 6 months with human parathyroid hormone (1-34) peptide in ovariectomized cynomolgus monkeys (*Macaca fascicularis*). Bone 25:301–309.

Kong YY, Yoshida H, Sarosi I, Tan HL, Timms E, Capparelli C, Morony S, Oliveira-dos-Santos AJ, Van G, Itie A, Khoo W, Wakeham A, Dunstan CR, Lacey DL, Mak TW, Boyle WJ, Penninger JM. 1999. OPGL is a key regulator of osteoclastogenesis, lymphocyte development and lymph-node organogenesis. Nature 397:315–323.

Kudo Y, Itatsu S, Iwashita M, Iguchi T, Takeda Y. 1995. Effects of estrogen and parathyroid hormone on osteoblastic activity via regulating the binding activity of insulin-like growth factor binding protein-4 in SaOS-2 cells: Implications for the pathogenesis of postmenopausal osteoporosis. Biochim Biophys Acta 1245:402–406.

Lane JM, Russell L, Khan SN. 2000. Osteoporosis. Clin Orthop 372:139–150.

Li M, Shen Y, Wronski TJ. 1997. Time course of femoral neck osteopenia in ovariectomized rats. Bone 20:55–61.

Lindsay R, Nieves J, Formica C, Henneman E, Woelfert L, Shen V, Dempster D, Cosman F. 1997. Randomised controlled study of effect of parathyroid hormone on vertebral-bone mass and fracture incidence among postmenopausal women on oestrogen with osteoporosis. Lancet 350:550–555.

Locklin RM, Khosla S, Turner RT, Riggs BL. 2003. Mediators of the biphasic responses of bone to intermittent and continuously administered parathyroid hormone. J Cell Biochem 89:180–190.

Manolagas SC, Jilka RL. 1995. Bone marrow, cytokines, and bone remodeling. Emerging insights into the pathophysiology of osteoporosis. N Engl J Med 332: 305–311.

Melton LJ III. 1997. The prevalence of osteoporosis. J Bone Miner Res 12:1769–1771.

Meng XW, Liang XG, Birchman R, Wu DD, Dempster DW, Lindsay R, Shen V. 1996. Temporal expression of the anabolic action of PTH in cancellous bone of ovariectomized rats. J Bone Miner Res 11:421–429.

Montero A, Okada Y, Tomita M, Ito M, Tsurukami H, Nakamura T, Doetschman T, Coffin JD, Hurley MM. 2000. Disruption of the fibroblast growth factor-2 gene results in decreased bone mass and bone formation. J Clin Invest 105:1085–1093.

Montgomery DC. 2001. "Design and analysis of experiments." New York: John Wiley & Sons.

Müller R, Van Campenhout H, Van Damme B, Van Der Perre G, Dequeker J, Hildebrand T, Rüegsegger P. 1998. Morphometric analysis of human bone biopsies: A quantitative structural comparison of histological sections and micro-computed tomography. Bone 23:59–66.

Nasu M, Sugimoto T, Kaji H, Chihara K. 2000. Estrogen modulates osteoblast proliferation and function regulated by parathyroid hormone in osteoblastic SaOS-2 cells: role of insulin-like growth factor (IGF)-I and IGF-binding protein-5. J Endocrinol 167: 305–313.

Neer RM, Arnaud CD, Zanchetta JR, Prince R, Gaich GA, Reginster JY, Hodsman AB, Eriksen EF, Ish-Shalom S, Genant HK, Wang O, Mitlak BH. 2001. Effect of parathyroid hormone (1-34) on fractures and bone mineral density in postmenopausal women with osteoporosis. N Engl J Med 344:1434–1441.

Parfitt AM, Drezner MK, Glorieux FH, Kanis JA, Malluche H, Meunier PJ, Ott SM, Recker RR. 1987. Bone histomorphometry: Standardization of nomenclature, symbols, and units. Report of the ASBMR Histomorphometry Nomenclature Committee. J Bone Miner Res 2:595–610.

Rao LG, Wylie JN, Sutherland MS, Murray TM. 1994. 17 beta-estradiol and parathyroid hormone potentiate each other's stimulatory effects on alkaline phosphatase activity in SaOS-2 cells in a differentiation-dependent manner. Endocrinology 134:614–620.

Reeve J, Meunier PJ, Parsons JA, Bernat M, Bijvoet OL, Courpron P, Edouard C, Klenerman L, Neer RM, Renier JC, Slovik D, Vismans FJ, Potts JT, Jr. 1980. Anabolic effect of human parathyroid hormone fragment on trabecular bone in involutional osteoporosis: A multicentre trial. Br Med J 280:1340–1344.

Rosen CJ, Bilezikian JP. 2001. Clinical review 123: Anabolic therapy for osteoporosis. J Clin Endocrinol Metab 86:957–964.

Rüegsegger P, Koller B, Müller R. 1996. A microtomographic system for the nondestructive evaluation of bone architecture. Calcif Tissue Int 58:24–29.

Samuels A, Perry MJ, Tobias JH. 1999. High-dose estrogen induces de novo medullary bone formation in female mice. J Bone Miner Res 14:178–186.

Shen V, Birchman R, Wu DD, Lindsay R. 2000. Skeletal effects of parathyroid hormone infusion in ovariectomized rats with or without estrogen repletion. J Bone Miner Res 15:740–746.

Simmons DJ. 1966. Collagen formation and endochondral ossification in estrogen treated mice. Proc Soc Exp Biol Med 121:1165–1168.

Sims NA, Morris HA, Moore RJ, Durbridge TC. 1996. Estradiol treatment transiently increases trabecular bone volume in ovariectomized rats. Bone 19:455–461.

Slovik DM, Neer RM, Potts JT, Jr. 1981. Short-term effects of synthetic human parathyroid hormone-(1-34)

administration on bone mineral metabolism in osteoporotic patients. J Clin Invest 68:1261–1271.
Turner RT, Kidder LS, Zhang M, Harris SA, Westerlind KC, Maran A, Wronski TJ. 1999. Estrogen has rapid tissue-specific effects on rat bone. J Appl Physiol 86: 1950–1958.
Walker-Bone K, Dennison E, Cooper C. 2001. Epidemiology of osteoporosis. Rheum Dis Clin North Am 27:1–18.
Westerlind KC, Wakley GK, Evans GL, Turner RT. 1993. Estrogen does not increase bone formation in growing rats. Endocrinology 133:2924–2934.
Zhou H, Shen V, Dempster DW, Lindsay R. 2001. Continuous parathyroid hormone and estrogen administration increases vertebral cancellous bone volume and cortical width in the estrogen-deficient rat. J Bone Miner Res 16:1300–1307.